ACADEMIA ROMÂNĂ
Revue Roumaine de Chimie
https://www.icf.ro/rrch/

Rev. Roum. Chim.,
2024, *69*(3–4), 119–127
DOI: 10.33224/rrch.2024.69.3-4.02

PRODUCTION AND ANTIOXIDANT ACTIVITY OF ELECTROSPUN POLYLACTIC ACID (PLA) NANOFIBROUS MATS CONTAINING NARINGENIN (NAR) FOR POTENTIAL WOUND HEALING APPLICATIONS

Serap AYAZ SEYHAN,[a,c,*] Zeynep ERDAG,[b] Sumeyye CESUR[c,d] and Dilek BILGIC ALKAYA[a,c]

[a]Marmara University, Faculty of Pharmacy, Department of Analytical Chemistry 34854, Basıbuyuk, Istanbul, Turkey
[b]Marmara University, Faculty of Pharmacy, 34854, Basıbuyuk, Istanbul, Turkey
[c]Center for Nanotechnology & Biomaterials Application and Research (NBUAM), Marmara University, Istanbul, Turkey
[d]Marmara University, Faculty of Technology, Metallurgical and Materials Engineering, Department of Ceramics, Istanbul, Turkey

Received January 23, 2023

In tissue engineering applications, the use of natural compounds without undesired side effects is highly preferred compared to chemical drugs. Flavonoids, polyphenolic compounds distributed widely in plant-based foods, exert diverse biological effects in cultured cells and in vivo. Flavonoids exhibit anti-inflammatory, antioxidant, anti-mutagenic, anti-cancerous, antiproliferative, and proapoptotic activities, enzyme modulating activities with minimal toxicity issues. Naringenin (4′,5,7-trihydroxyflavanone) (NAR) is a flavonoid belonging to the class flavanone, predominantly found in grape fruit, bitter orange, and other citrus fruits. It has very prominent pharmacological actions like antitumor, vasoprotective, antihypertension, antiviral, and dantishockactions. As NAR can scavenge reactive oxygen species, its use in wound dressing studies is increasing. In recent years, many studies have been carried out to produce nanofibrous materials by the electrospinning method. Electrospun nanofibers have very large surface areas, controllable pore sizes, and tunable drug release profiles. Several biocompatible polymers with excellent biocompatibility and biodegradability including polylactic acid (PLA) have been widely used for the synthesis of nanofibers using the electrospun technique. In this study, nanofibers were obtained by adding NAR at different concentrations into PLA by electrospinning technique. Morphological (Scanning electron microscopy, SEM), molecular interaction (Fourier transform infrared spectroscopy, FT-IR), thermal analysis (Differential scanning calorimetry, DSC), antioxidant activity, and physical analysis were carried out after the production process. Meanwhile, the PLA nanofibers showed the largest swelling value of 220% after immersion in phosphate buffer saline (PBS) solution for 10 days. Overall, this study demonstrates that our PLA/NAR nanofiber mats are attractive candidates for wound dressing material research and application.

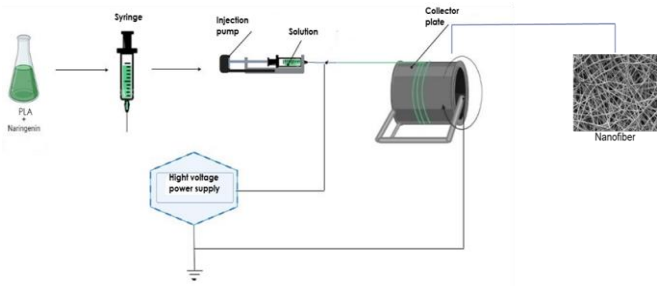

INTRODUCTION

There are many poorly soluble or hydrophobic bioactive compounds and nutrients which are essential for human health, such as essential oils, carotenoids, essential fatty acids, phenolic compounds, and insoluble vitamins. The sustainability and low bioavailability of these compounds are the main challenges for their use in the pharmaceutic and food industries.[1]

* Corresponding author: sayaz@marmara.edu.tr

Flavonoids, polyphenolic compounds distributed widely in plant-based foods, exert diverse biological effects in cultured cells and in vivo. Flavonoids exhibit antioxidant, anti-cancerous, anti-mutagenic, anti- inflammatory effects.[2] Naringenin (NAR) is a bioactive flavonoid found in grapes and citrus fruits including tangelo, blood orange, lemons, and tangerines using different extraction and hydrolysis methods.[3] It is considered to have a bioactive effect on human health as an antioxidant, free radical scavenger, anti-inflammatory, carbohydrate metabolism promoter, and immune system modulator. This substance has also been shown to repair DNA.[4,5] The NAR is proposed to have pharmacologically significant effects against chronic diseases including diabetes, hypertension, inflammation, and allergy.[6–10] Besides, that NAR works synergistically with anticancer drugs, especially in resistant cancer forms. Finally, as NAR can scavenge reactive oxygen species, its use in wound dressing studies is increasing.[11]

The skin is the largest organ of the body, classified as soft tissue. It is responsible for retaining moisture, regulating the body temperature, protecting against microbes and harmful external observations such as wounds, burns, and trauma, and transmitting the senses.[12] The skin has regenerative properties, but the healing process is difficult in heavy intense injuries and deep wounds.[13] Wound dressings have an important function in promoting the healing of certain types of wounds.[14] Nowadays, polymeric nanofibers have brought an alternative perspective to existing wound treatments. These fibers, which have features such as ultra-thin structure and large surface area, attract the attention of researchers and are used in applications. There are many methods for the production of nanostructure fibers such as freeze-drying, electrospinning, and 3D printing. Among them, electrospinning is the easiest and most convenient method.[15] Electrospinning is a widely used technique to produce fibers with diameters in the range of a few micrometers to several hundred nanometers from polymer solutions or melts. Polymer solution, sprayed from a jet, converts into nanofiber under an electric field. Nanofiber formation depends on voltage, flow rate, type of collector, the distance between needle and collector, and solution.[16] Fibers for use as wound dressings have a high surface-to-volume ratio that ensures the continuous diffusion of drug molecules. Also, electrospun nanofibers can provide the necessary environment for antioxidant encapsulation. It was reported that NAR, a hydrophobic drug molecule, exhibits more effective activity through controlled release when used in combination with nanofiber structures.[17–19] Moreover, NAR-loaded nanoparticles have also been widely investigated for various applications. Natural and synthetic nanofibers produced from polymers are promising in wound treatments as drug delivery systems. Among the polymers used as a matrix for the electrospinning process, synthetic poly (lactic acid) was the most widely used Polylactic acid (PLA) is a biodegradable, biocompatible, and ecological polymer. It is also preferred because of its non-toxicity, good oxygen permeability, and drug-loading efficiency.[20] It does not cause any damage in contact with the skin. Therefore, tissue science and wound dressing are widely used.

In medicine, the care of infected or uninfected wounds such as diabetes, cancer, and allergies can be activated via antioxidant compounds such as free radical scavenging agents. However, the disadvantage is that external factors such as pH, temperature, or exposure to light cause the bioavailability and bioaccessibility of antioxidants to degrade these compounds.[21] Consequently, antioxidants can encapsulate to enhance their availability, thereby maintaining their properties. Therefore, this study aimed to develop a biomaterial-based nanofibrous wound dressing containing NAR by adding NAR at different concentrations into PLA by electrospinning technique. Morphological (SEM), molecular interaction (FT-IR), mechanical analysis, thermal analysis (DSC), and physical analysis of total phenolic content and antioxidant activity were carried out after the production process.

RESULTS AND DISCUSSION

In this study, NAR, whose pharmacological effect has been proven by many studies[19,22] was encapsulated in polymeric nanofibers in order to improve its therapeutic effect and pharmacokinetics.

Morphology of electrospun nanofibers

Processing parameters such as applied voltage, the distance between needle and collector, solution flow rate, temperature, and relative humidity affect the transformation of polymer solutions into fibers in the electrospinning process.[23] The surface morphologies of the produced nanofibers were analyzed using SEM. SEM images and diameter distributions are shown in Fig. 1. It was seen that homogeneous and smooth nanofibers were obtained without any beading both drug-loaded and unloaded nanofibers. The mean diameters of,

PLA, PLA//8NAR, PLA/16NAR and PLA/40NAR electrospun nanofibers were; 854.9 ±130.6 nm; 907.5 ±124.8 nm; 899.2 ± 112.1 nm; 883.7 ± 130.3 nm respectively. A decrease in diameter of nanofibers was observed when NAR was loaded into pure nanofibers. As the NAR ratio increased, the diameter further decreased (Fig. 1). As other researchers have noted, drug loading into the electrospinning solution affects electrical conductivity and viscosity. This leads to an increase in the size of the nanofibers and the formation of larger-diameter nanofibers.[24,25]

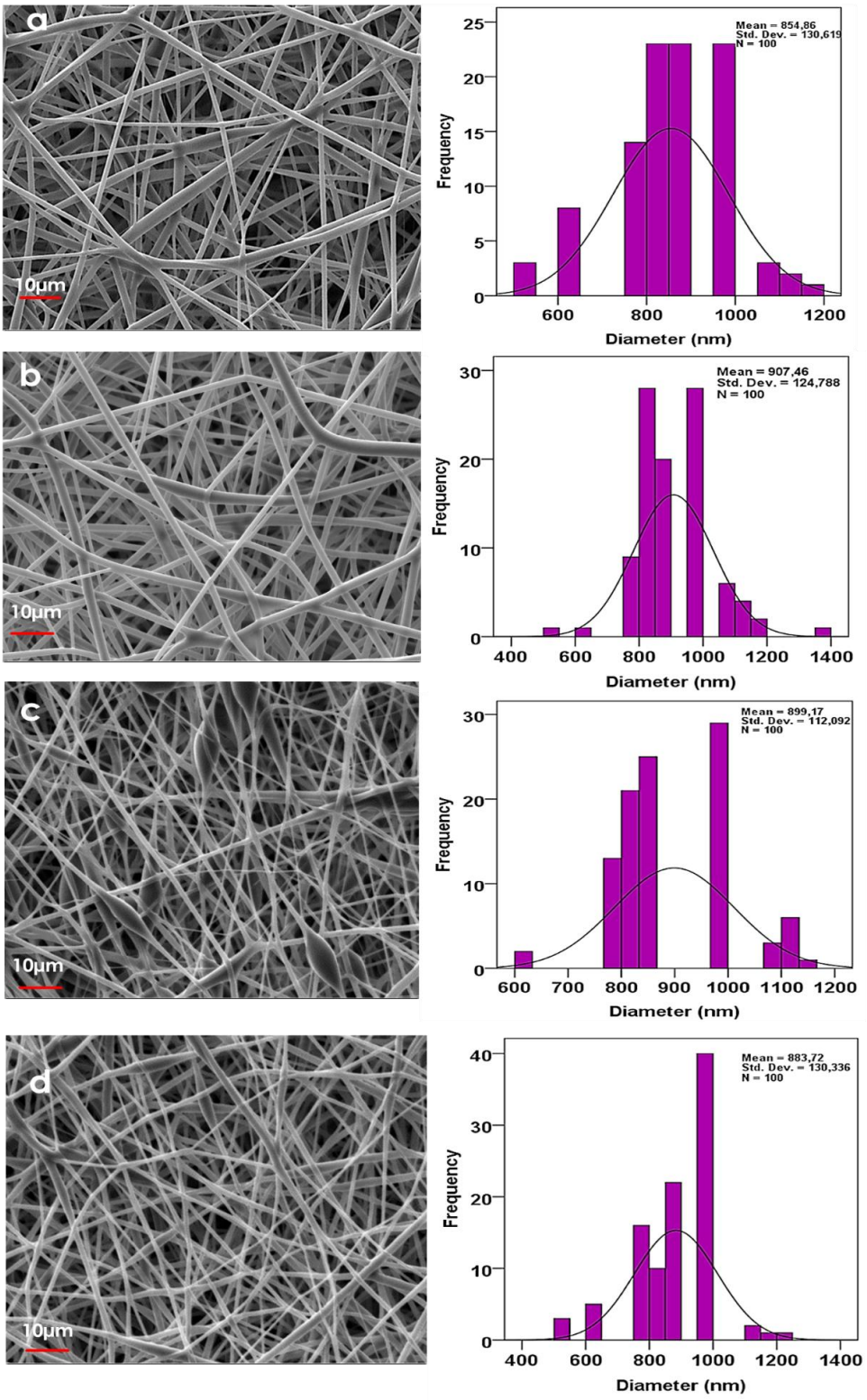

Fig. 1. – SEM images and fiber diameter distribution of: a) Pure PLA; b) PLA/8NAR; c) PLA/16NAR; d) PLA/40NAR.

Fourier transform infrared spectroscopy

The chemical group transformation and the spectra for PLA/NAR loaded electrospun nanofibers were investigated by FT-IR spectroscopy. The results of the FTIR analysis of the molecular structure are shown in Fig. 2. The structure of NAR contains 5-hydroxyl and 4-carbonyl group and therefore, it form potential intramolecular hydrogen bonds.[26] As can be seen, the spectra of pure NAR produced the characteristic peaks carbonyl absorption band around 1700 cm^{-1} (C=O, stretching) assigned to aromatic ketonic carbonyl stretching. The spectra of pure NAR exhibited characteristic peaksat 3400 cm^{-1} (OH, stretching), 1550–1600 cm^{-1} (C=C in the aromatic ring, stretching), 1519 cm^{-1} (C–C in the ring, stretching), 1008 cm^{-1} (C–O, stretching). The strong band at 832.1 cm^{-1} corresponded to para-disubstituted benzene, reflecting the structure of NAR.[27,28] The characteristic peak of PLA are C=O vibration peak at 1750 cm^{-1}, CH_3 asymmetric shear at 1456 cm^{-1}, CH_3 and C–H bending vibrations 1386 and 1358 cm^{-1}, C–O–C stretching vibration at 1265 cm^{-1}, C-O and C–O–C stretching at 1080 cm^{-1}, C–CH_3 stretching, OH bending at 950 cm^{-1} and C–COO stretching at 873 cm^{-1}.[24,29] After the incorporation of NAR powder in PLA nanofibers, -OH stretching band at 3400 cm^{-1} disappeared. This demonstrated the formation of a new intermolecular hydrogen bond between NAR and the backbone chain of PLA, and the homogeneous incorporation of NAR over the polymer's matrices. Moreover, the characteristic peaks of PLA (3500cm^{-1} and 1750 cm^{-1}) was observed in the PLA/NAR nanofibers.

Also, the peak shift in the fingerprint region (C-O and C–O–C stretching at 1080 cm^{-1}, and C–COO stretching at 873 cm^{-1}) can be explained by the possible hydrogen bonding between NAR and PLA. These changes, including disappearance or shifting of wave numbers of particular peaks indicates that the NAR was successfully encapsulated in the polymer.

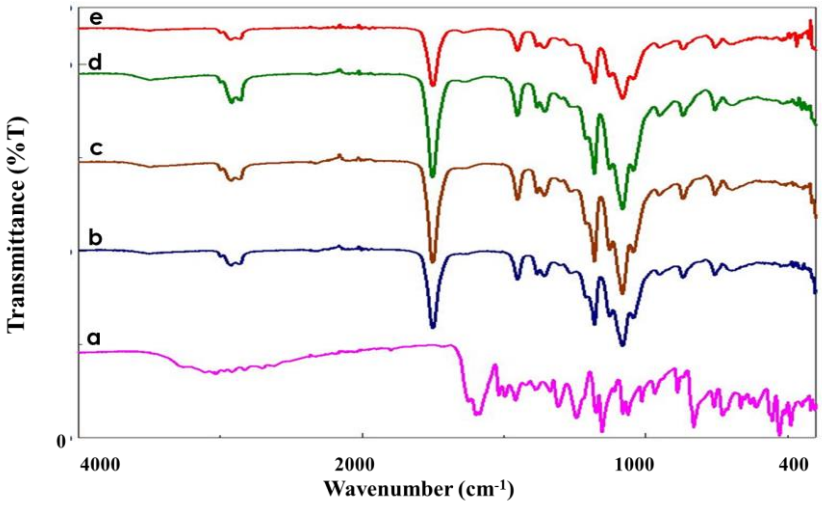

Fig. 2. – FTIR spectra of the: a) NAR; b) PLA; c) PLA/8NAR nanofiber; d) PLA/16NAR nanofiber; e) PLA/40NAR nanofiber.

Differential scanning calorimetry analysis

In the thermogram obtained as a result of the thermal analysis using a differential scanning calorimeter device, sharp endothermic peaks were observed indicating that the crystal structure of the polymer chains was disrupted. These peaks indicate the melting curve of polymers. The main thermal transitions and heating processes of the electrospun nanofibers were analyzed by DSC, respectively, as shown in Fig. 3. The first heat, in this instance, shows a small glass transition (Tg) around 60 °C with some cold crystallization beginning around 90 °C and a melt with a peak temperature of about 150°C. DSC results indicate that while cold-crystallization is in a highly amorphous form in pure PLA, the decreased cold-crystallinity is associated with the increase of the NAR ratio. The loading of NAR extract on PLA electrospun nanofibers affected the molecular chain mobility and caused a change in the thermal behavior of the material.[27] These findings are in good agreement with experimental results obtained for morphological and mechanical tests of the mats.

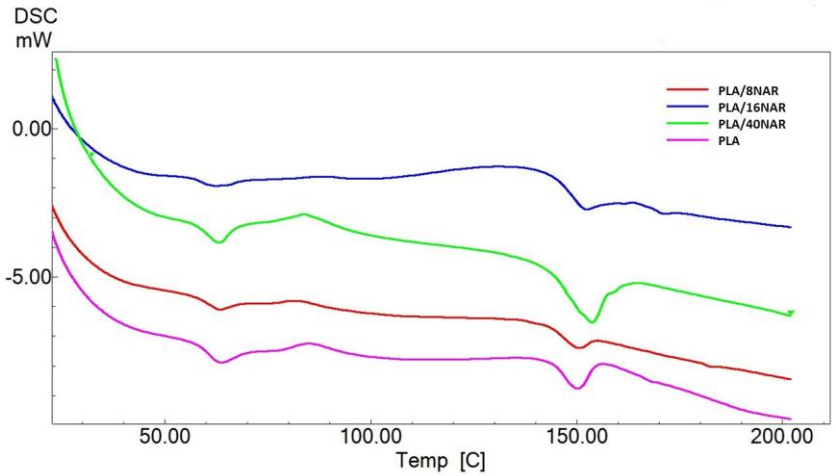

Fig. 3. – DSC thermogram of pure PLA and NAR-loaded nanofibrous mats in three different concentrations (8, 16, and 40 mg).

Mechanical Properties

The tensile strength and strain at break for each nanofiber sample are indicated in Fig. 4. When we look at the tensile strength and strain at break measurement results, when NAR was added to the PLA, it was observed that strain at break values increased proportionally with the concentration of NAR. Similar results were also seen in the strain at break. From Fig. 4, it can be seen that PLA/40NAR fiber exhibited a large elongation at break.[30] Therefore, this fiber has a ductile nature. These results exhibited that the incorporation of 40NAR highly increased the elasticity of PLA.

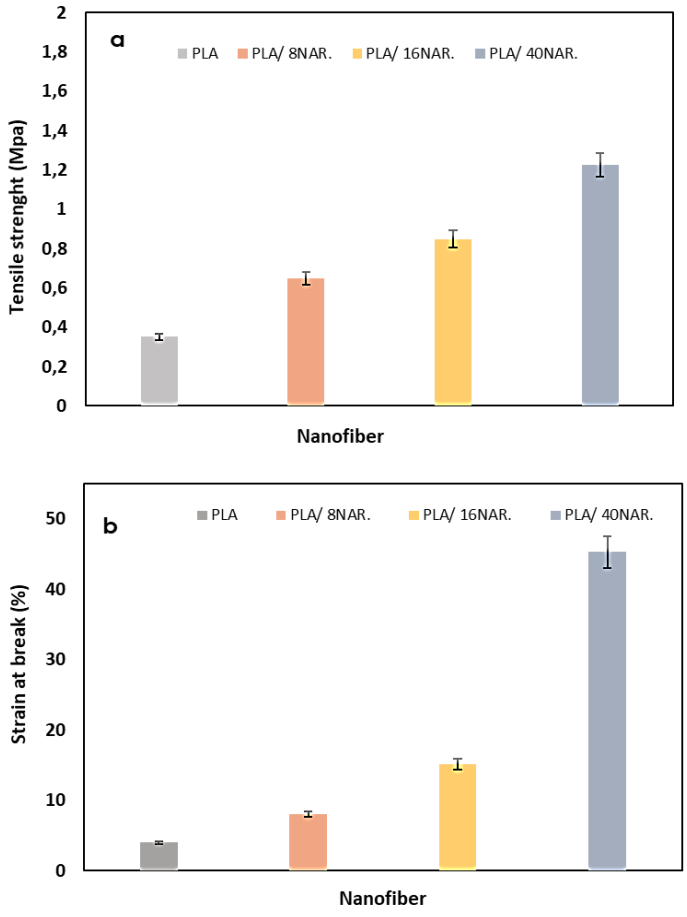

Fig. 4. – Physical parameters of nanofiber mats: a) tensile strenght; b) strain at break.

Swelling Study

In order to understand the liquid absorption capacity of PLA nanofibers, the swelling test was performed in a PBS medium. Figure 5 shows the time-dependent swelling percentages of electrospun PLA. As shown in Fig. 5, there is a high swelling ratio in the first phases of all samples. After 10 days, the highest swelling rate was observed on PLA/40NAR electrospun nanofiber, reaching up to 220 %.

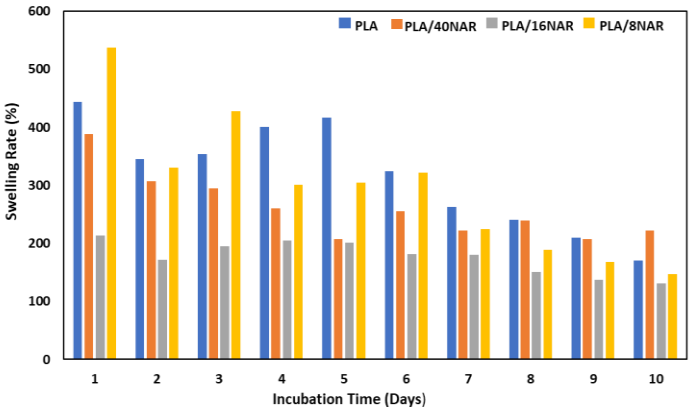

Fig. 5. – Swelling kinetics of NAR/PLA nanofiber mats in PBS 7.4 at 37 ºC.

Phenolic content and antioxidant properties

The total phenolic content of NAR- loaded nanofibers was determined with Folin-Ciocalteu reagent and free radical scavenging activity of electrospun nanofibers was determined using DPPH radical. The purple color of the DPPH solution is due to unpaired electrons in the structure. If an antioxidant molecule enters the medium, hydrogen is bound to the DPPH molecule instead of the free electron. Consequently, the color of the solution changes from purple to yellow or colorless depending on the decrease in absorbance.[31] In Fig. 6, it is seen that PLA (control) has very weak, while PLA/NAR fibers exhibit significant antioxidant activity. This indicates that exposure to high voltage during the electrospinning process does not affect the antioxidant activities. Similar results were also seen in the total phenolic content. As expected, pure PLA did not show any antioxidant effect. However, it served as a reservoir and protection system for the antioxidants found in the NAR investigated.[32]

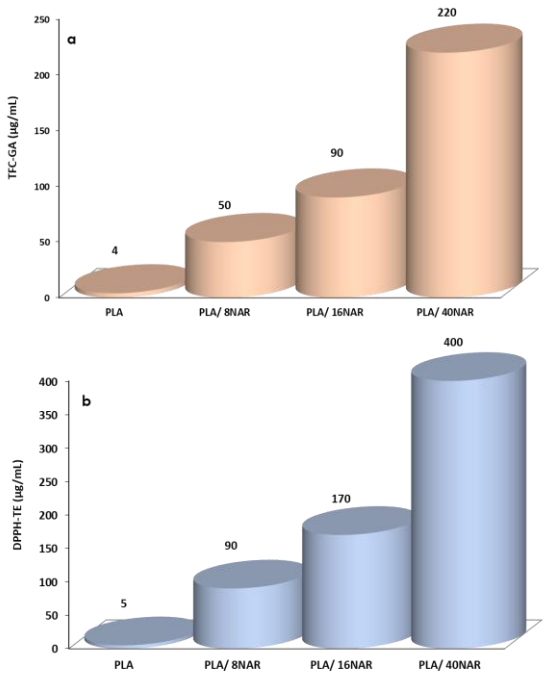

Fig. 6. – Total phenolic content and antioxidant activity of nanofiber mats: a) Folin-Ciocalteu reagent; b) DPPH· Radical.

EXPERIMENTAL

Materials

Polylactic acid (PLA) 2003D was purchased from Nature Works LLC, Minnetonka, MN. Acetic acid (CH_3COOH), Chloroform and Tween 80 (viscous liquid), Citric acid, 1,1-Diphenyl-2-picrylhydrazyl radical (DPPH); 6-hydroxy-2,5,7,8-tetramethylchroman-2-carboxylic acid (Trolox); 2,4,6-tri(2-pyridyl)-s-triazine (TPTZ), Folin-Ciocalteu phenol reagent, gallic acid (GA), naringenin (NAR), Trolox (6-hydroxy-2,5,7,8-tetramethylchroman-2-carboxylic acid), sodium carbonate, PBS (phosphate-buffered saline) pH 7.4 solution were purchased from Sigma- Aldrich Co. (St. Louis, MO, USA).

Preparation and Characterization of Electrospinning Solutions

Naringenin (NAR) was dissolved in three different concentrations (8 mg/mL, 16 mg/mL, and 40 mg/mL) in ethanol. PLA was dissolved in chloroform at magnetic stirring (IKA, RCT, Germany) for about 2 h to obtain the concentration of 8 % (w/v) at room temperature. Then 3 % by weight of Tween 80 was added to the PLA solution and mixed for an additional 15 minutes. NAR solutions (1mL) prepared in ethanol at different concentrations were added to the PLA/Twin 80 mixture and this solution was stirred for 20 minutes, separately. All nanofibers were produced by electrospinning at ambient conditions (25 ºC).

Fabrication of Electrospun Nanofibers

The electrospinning method was utilized for the fabrication of electrospun nanofibers. The experimental setup composes a syringe pump (NE-300, New Era Pump Systems, Inc., USA), a single brass needle (diameter of 1.63 mm), a high voltage power supply connected to the needle, and a laboratory scale electrospinning unit (NS24, Inovenso Co., Turkey). The homogeneous polymer solutions were filled into 10 mL plastic syringes. For electrospinning, the solutions were delivered with a constant flow rate of 2 mL/h using a syringe pump. Electrospun nanofibers were produced at 25 kV, a 12 cm distance between the collector and needle, and a 1 mL/h flow rate. Collector's rotating speed was adjusted to 100 revolutions per minute. All the experiments were performed at ambient conditions (25 ºC) and humidity (40–45 %).[33]

Scanning Electron Microscopy

The morphology of nanofibers was observed by scanning electron microscope (SEM) (EVO LS 10, Zeiss, Germany) after being coated with gold-palladium for 120 seconds. The applied accelerating voltage was 12 kV. The diameters of the electrospun nanofibers were measured by the image analysis software (Olympus AnalySIS, USA) by choosing 100 fibers from each SEM image randomly. The collected data were transferred to SPSS software for further analysis.

Fourier Transform Infrared Spectroscopy (FTIR)

Fourier-transformed infrared spectroscopy (FTIR) analysis was used to qualitatively characterize the functional groups of electrospun nanofibers (Jasco FT/ IR-4700, Japan). Each spectrum was recorded between 4000 and 400 cm^{-1} and averaged over 32 scans with 4 cm^{-1} resolution.

Differential Scanning Calorimetry (DSC)

The main thermal transitions and the heating runs of electrospun nanofibers were analyzed by DSC (Shimadzu DSC-60 Plus, Japan). Temperature ranges were adjusted from 25 ºC to 300 ºC for all electrospun nanofiber groups (scanning rate of 10 ℃/min).

Mechanical Properties

Before the testing, each different sample was sectioned into five rectangular-shaped samples which are 5 cm in length and 1 cm in width, and the thickness of the nanofibrous meshes of different types was calculated using a digital micrometer (Mitutoyo MTI Corp., USA). The mechanical properties were analyzed with a tensile testing machine (Shimadzu Corporation, EZ-LX, Kyoto, Japan). The test speed was adjusted to 5 mm/min, and a 5 kN load was applied during the test. For each group, three different samples were tested.

Swelling Study

Electrospun nanofibers were cut into 3 pieces of that same weight. These pieces were dipped into PBS buffer (pH: 7.4) at 37 ℃ and placed in a thermal shaker (BIOSAN TS-100, Biosan Riga, Latvia). They were removed from the buffer solution at certain time intervals and pressed onto the blotter to absorb excess liquid.[34] They were weighed and their swelling rates were determined using equation.[35]

$$S= (Ww-Wo)/Wo.100$$

Total Phenolic Content

The total polyphenols content of NAR-loaded nanofibers was determined by Folin Ciocalteu method.[36] Firstly, nanofiber samples (0,01g) were extracted with %70 ethanol (v/v) using an orbital shaker-incubator (BIOSAN ES-20, Biosan Riga, Latvia) at a constant stirring speed (200 rpm, at 37 °C) for 1 hour. Briefly, 100 µL of each sample was mixed with 4 mL water and 100 µL of Folin-ciocalteu reagent. Then, 100 µL of sodium carbonate (6%) was added to each sample. The absorbance was measured between 685–760 nm after 30 min reaction by using a spectrophotometer (Shimadzu UV-1601, Japan). The calibration curve was prepared using gallic acid standard, in the concentration range of 62.5–1000 µg/mL ($y = 0.0018\ x – 0.0135$, $r^2 = 0.9992$). Results were expressed as gallic acid equivalents (GAE/mL). All measurements were repeated three times.

Determination of Radical Scavenging Ability by Using DPPH Method

DPPH radical scavenging activity of NAR-loaded electrospun nanofibers was determined according to Ayaz Seyhan.[37] Briefly, 1.5 mL DPPH of each sample was mixed with 1,5 mL $DPPH^{\cdot}$ radical solution (100µM) using an orbital shaker-incubator (BIOSAN ES-20, Biosan Riga, Latvia) at a constant stirring speed (200 rpm, at 37 °C) for 30 min. The absorbance was measured between 515–528 nm by using a spectrophotometer (Shimadzu UV-1601, Japan). The calibration curve was prepared using the trolox standard, in the concentration range of 0.625–8.76 µg/mL ($y = –0.0606\ x$ + + 0.6205, $r^2 = 0.9932$). Results were expressed as trolox equivalents (TE/mL). All measurements were repeated three times.

Statistical analysis

The statistical analyzes of the data obtained as a result of the measurements were made using a single-factor ANOVA analysis program. Diameter measurements of electrospun nanofibers were made using SPSS analysis program. All results are given as the mean ± STD. Statistical significance was defined as $p < 0.05$.

CONCLUSIONS

In this study, PLA, PLA/8NAR, PLA/16NAR and PLA, PLA/40NAR electrospun nanofibers were successfully produced by electrospinning for wound dressing applications. The morphological, chemical, thermal, and mechanical properties of all fiber samples formed by the electrospinning method were examined and the results were evaluated. Characterization tests showed that different concentrations of NAR were successfully loaded on PLA electrospun nanofibers by the electrospinning method. Characteristic chemical bonds of PLA were observed in the FTIR analysis, confirming successful fiber production. When the SEM images of the electrospun nanofibers were examined, it was seen that they have a smooth structure without beads and that they were no observed drug crystals and clusters on the surface. The tensile test observed that adding NAR to the PLA combination increased the stress at break. As a result of thermal characterization, it has been shown that the fibers can be used at body temperature (35–38 °C) without any degradation or phase change. Considering the antioxidant activity results, while PLA did not show any antioxidant effect, it was observed that the antioxidant activity increased with the concentration of NAR ratio in the nanofibers. When all the results are evaluated, electrospun nanofibers containing NAR may have promising potential in wound dressing applications.

REFERENCES

1. J. Muñoz, M. C. Alfaro, L. A. Trujillo-Cayado, J. Santos and M. J. Martín-Piñero, "Nanoencapsulation of Food Ingredients by Specialized Equipment", Academic Press, United Kingdom, 2019, p. 341–390.
2. J. H. Lee, C. H. Park, K. C. Jung, H. S. Rhee and C. H. Yang, *Biochem. Biophys. Res. Commun*., **2005**, *335*, 771–776.
3. J. Stabrauskiene, M. Marksa, L. Ivanauskas and J. Bernatoniene, *Pharmaceutics*, **2022**, *14*, 890–898.
4. K. A. Youdim, M. Z. Qaiser, D. J. Begley, C. A. Rice-Evans and N. J. Abbott, *Free Radic. Biol. Med*., **2004**, *36*, 592–604.
5. J. K. Prasain, S. H. Carlson and J. M. Wyss, *Maturitas*, **2010**, *66*, 163–171.
6. K. Patel, G. K. Singh and D. K. Patel, *Chin. J. Integr. Med*., **2018,** *24*, 551-560.
7. S. Md, N. A. Alhakamy, H. M. Aldawsari, M. Husain, S. Kotta, S. T. Abdullah, U. A. Fahmy, M. A. Alfaleh and H. Z. Asfour, *Pharmaceuticals*, **2020**, *13*, 152–158.
8. P. Parashar, M. Rathor, M. Dwivedi and S. A. Saraf, *Pharmaceutics*, **2018**, *10*, 33–40.
9. S. Jacob and A. B. Nair, *Drug Dev. Res*., **2018**, *79*, 201–217.
10. S. H. Akrawi, B. Gorain, A. B. Nair, H. Choudhury, M. Pandey, J. N. Shah and K. N. Venugopala, *Pharmaceutics*, **2020**, *12*, 893–900.
11. Z. Memariani, S. Q. Abbas, S. S. Ul Hassan, A. Ahmadiand A. Chabra, *Pharmacol. Res.*, **2021**, *171*, 105264–105270.
12. M. Foroutan Koudehi and R. Zibaseresht, *Materials Technology*, **2020**, *35*, 21-30.
13. J. Ahlawat, V. Kumar and P. Gopinath, *Mater. Sci. Eng.: C*, **2019**, *103*, 109834–109840.
14. H. R. Bakhsheshi-Rad, Z. Hadisi, A. F. Ismail, M. Aziz, M. Akbari, F. Berto and X. B. Chen, *Polymer Testing*, **2020**, *82*,106298–106304.
15. V. Kumar, S. Naqvi and P. Gopinath, "Applications of nanomaterials", Woodhead Publishing, 2018, p. 179-203.
16. C. J. Angammana and S. H. Jayaram, *Part. Sci. Technol*., **2016**, *34*, 72-82.
17. P. Zhang, X. Liu, W. Hu, Y. Bai and L. Zhang, *Carbohydrate Polymers*, **2016**, *149*, 224-230.
18. Q. Zhang, Y. Zhang, D.C. Watts, H.N.S. Almassri, H. Shao, X. Yang, Y. Ma, D. Zhang and X. Wu, *Sci. Adv. Mater.*, **2019**, *11*, 1433-1442.
19. M. Bhia, M. Motallebi, B. Abadi, A. Zarepour, M. Pereira-Silva, F. Saremnejad, A. C. Santos, A. Zarrabi, A. Melero and S. M. Jafari, *Pharmaceutics*, **2021**, *13*, 291–306.
20. S. Cesur, M. E. Cam, F. S. Sayin and O. Gunduz, *J. Drug Deliv. Sci. Technol*., **2022**, *67*, 102977–102306.
21. A. Vilchez, F. Acevedo, M. Cea, M. Seeger and R. Navia, *Nanomaterials*, **2020**, *10*, 175–182.
22. B. Salehi, P. V. T. Fokou, M. Sharifi-Rad, P. Zucca, R. Pezzani, N. Martins, J. Sharifi-Rad, *Pharmaceuticals*, **2019**, *12*, 11–18.
23. R. E. Ghitescu, A. M. Popa, V. I. Popa, R. M. Rossi and G. Fortunato, *Int. J. Pharm*., **2015**, *494*, 278-287.
24. M. E. Cam, S. Cesur, T. Taskin, G. Erdemir, D. S. Kuruca, Y. M. Sahin, L. Kabasakal and O. Gunduz, *Eur. Polym. J*., **2019**, *120*, 109239–109244.
25. S. Cesur, *Konya J. Engineer. Sci*,, **2022**, *10*, 878-888.
26. M. H. Akhter, S. Kumar and S. Nomani, *Drug Dev. Ind. Pharm.*, **2020**, *46*, 659-672.
27. R. L. Nagula and S. Wairkar, *Int. J. Biol. Macromol.*, **2020**, *164*, 717–725.
28. S. Maity and A. S. Chakraborti, *Eur. Polym. J.*, **2020**, *134*, 109818–109824.
29. E. Saylam, Y. Akkaya, E. Ilhan, S. Cesur, E. Guler, A. Sahin, E. Cam, N. Ekren, F. Nuzhet Oktar, O. Gunduz, D. Ficai, A. Ficai, P. Calandra and D. Lombardo, *Appl. Sci.*, **2021**, *11*, 10727–10734.

30. S. C. Wong, A. Baji and S. W. Leng, *Polymer*, **2008**, *49*, 4713–4722.
31. I. G. Munteanu and C. Apetrei, *Int. J. Mol. Sci.*, **2021**, *22*, 3380–3388.
32. I. Sriyanti, D. Edikresnha, A. Rahma, M. M. Munir and H. Rachmawati, *J. Nanomater*., **2017,** *2017*, 9687896–9687902.
33. M. E. Cam, B. Ertas, H. Alenezi, A. N. Hazar-Yavuz, S. Cesur, G. S. Ozcan, C. Ekentok, E. Guler, C. Katsakouli, Z. Demirbas, D. Akakin, M. S. Eroglu, L. Kabasakal, O. Gunduz and M. Edirisingh, *Mater. Sci. Eng. C-Mater. Biol. Appl.*, **2021**, *119*, 111586–111594.
34. Z. Guo, C. Yang, Z. Zhou, S. Chen and F. Li, *RSC Advances*, **2017**, *7*, 34063–34070.
35. S, Kaya and S. Derman. *Sigma J. Eng. Nat. Sci.*, **2022**, *40*, 433–440.
36. D. Çıkla Yılmaz and S. Ayaz Seyhan, *Istanbul J. Pharm.*, **2017**, *47*, 9–12.
37. S. A. Seyhan, *Batman Univ. J. Life Sci.*, **2019**, *9*, 125–135.